

Precise measurement of the β decay and electron capture of ^{22}Na , ^{198}Au , and ^{196}Au in low-temperature metal hosts, and reexamination of lifetime modifications

Götz Ruprecht,^{*} Christof Vockenhuber, Lothar Buchmann, Russell Woods, Chris Ruiz, and Suzanne Lapi[†]
TRIUMF, 4004 Wesbrook Mall, Vancouver, British Columbia, V6T 2A3, Canada

Daniel Bemmerer

Forschungszentrum Dresden-Rossendorf, Bautzner Landstr. 128, D-01328 Dresden, Germany

(Received 29 February 2008; published 18 June 2008)

We investigated half-life changes with temperature of ^{22}Na embedded in Al and $^{198}\text{Au}/^{196}\text{Au}$ embedded in Au. We do not find any change of the half-life between room temperature and 10 K on the level of 0.04% for ^{22}Na , 0.03% for ^{198}Au , and 0.5% for ^{196}Au in striking disagreement with the first experimental works and predictions. Additionally, the absolute half-life for ^{198}Au has been determined to 2.6937 ± 0.0003 d which is 5 standard deviations below the recommended NIST value but in agreement with other high-precision measurements.

DOI: [10.1103/PhysRevC.77.065502](https://doi.org/10.1103/PhysRevC.77.065502)

PACS number(s): 23.40.-s, 21.10.Dr, 27.30.+t

I. INTRODUCTION

Recently it has been suggested that half-lives of radioactive isotopes may change by orders of magnitude if they are embedded in a metal lattice and cooled to temperatures of a few Kelvin [1–5]. The predictions [1–5] are based on the Debye-Hückel model and are supported by reported half-life changes of up to 4% between room temperature and 4 K for the radionuclides ^{22}Na [6] (90% β^+ decay), ^{198}Au [7] (100% β^- decay), and ^{210}Po [8] (α decay) embedded in a metal. As the effect is suggested to increase with decreasing temperature it would be a possibility to change the half-lives of radioisotopes by orders of magnitude by adjusting the temperature. Consequently, it was proposed as a method of radioactive waste disposal [5].

The result for ^{198}Au is also important for neutron experiments where the $^{197}\text{Au}(n, \gamma)$ reaction and the subsequent ^{198}Au activity measurement is used to normalize the neutron flux. Therefore, if the ^{198}Au half-life was temperature dependent the results of many neutron induced measurements might have to be revised.

We will explain the theoretical background on which the predictions are based on and why these models cannot be used for low-temperature metal hosts. We then present our own measurements with a setup where special care was taken on the mechanical stability of the source as well as dead-time issues of the data acquisition system (DAQ).

II. THE SCREENING EFFECT

Reactions between two charged nuclei at low energy E are dominated by the probability of tunneling through the Coulomb barrier. This probability, called the penetrability $P(E)$, has an exponential-like energy dependence which drops

strongly toward lower energies. However, at energies close to the binding energy of atomic electrons, the slight reduction (screening) of the Coulomb potential caused by the electrons can have a remarkable effect on the penetrability, enhancing the cross section by orders of magnitude compared with that of fully ionized atoms. This effect, known as the electron screening effect [9], can be described by one single parameter, the screening energy $U_e = Z_1 Z_2 e^2 / R$, where Z_1 and Z_2 are the charge numbers of the two nuclei involved. The screening length R describes the size of the electron cloud which depends on the electronic environment the two nuclei are reacting in. As a first-order correction, the screening energy is then just added to the kinetic energy of the projectile to obtain the screening-enhanced cross section.

A general framework to derive U_e in different environments was published by Salpeter in 1954 [9]. It classifies the screening effect by the ratio of R to the mean distance a between the ions. For $R \gg a$, a so-called weakly coupled plasma, the electron screening can be well described by the *Debye-Hückel model* [10], developed 1923 by Debye and Hückel to explain the behavior of ions in a chemical solution. It is based on pure classical physics and as a result, U_e is dependent on the plasma temperature T by $U_e \sim 1/\sqrt{T}$ (Debye screening). As the plasma cools down, the electron cloud contracts. The temperature dependence becomes weaker and finally vanishes for $R \ll a$ (strongly coupled plasma). An extreme case of the latter condition is a metal lattice where the outer electrons are in the state of a degenerate Fermi gas. Under these circumstances, the screening energy depends only on the Fermi energy and density of the electrons but not explicitly on the temperature. A model for the transition between weakly and strongly coupled plasma has recently been proposed [11].

For a long time, the screening effect was believed to be understood and its influence to be small, until measurements in 1998 indicated that U_e is about one order of magnitude larger when the reacting nuclei are embedded into some metals [12]. Since then, several groups have investigated this “enhanced screening effect”, both experimentally and theoretically (see [13] and references therein), but no consistent explanation can

^{*}ruprecht@triumf.ca

[†]Present address: University of California, 185 Berry Street, San Francisco, CA 94107, USA.

be provided yet. In general, U_e is high for metals but no clear dependence on the properties of the host metal has been found so far.

Regardless of the origin of the high screening values in metals it is justified to assume that also the decay rate and therefore the half-life of radioactive nuclei should change when they are implanted in metals. The charged α and β particles also have to penetrate the Coulomb barrier modified by the electrons in the same manner as they do for nuclear reactions. However, as pointed out by Zinner [14] the effect is much smaller for decay as it is for reactions because the penetration enhancement is partially canceled by a slightly changed decay Q-value. The most sensitive dependence on U_e can be expected for α emitters with the lowest energies but they also have the lowest activities.

III. TEMPERATURE DEPENDENCE AND PREVIOUS MEASUREMENTS

Despite the limitation of the Debye-Hückel model to high temperatures (typically $> 10^5$ K for metals) a temperature dependence of U_e was investigated in $d + d$ reactions [1,15] as well as in decay experiments [6–8]. In Ref. [1], $d + d$ fusion reactions with the deuterons embedded in copper, platinum, and titanium in a temperature range between 260 K to 610 K have been measured. No clear temperature dependence of the screening energy could be observed, only a correlation with the solubility of the deuterons in the corresponding metals. In Ref. [15], the host metal was cooled all the time, therefore no comparison between different temperatures was made (see [16] for a detailed discussion). Here, we focus on a possible temperature dependence of the decay of radionuclides. The published results as well as the predictions from the Debye-Hückel model are summarized in Table I.

The prediction based on the Debye-Hückel model has been calculated as follows: From the $d + d$ measurements in different host metals [17], a typical screening value of $U_{d+d} = 300$ eV for room temperature has been adopted. This value has to be scaled by the product of the charge numbers of the ejectile Z_1 and the daughter nucleus Z_2 , $U_e = Z_1 Z_2 U_{d+d}$ (note that U_e becomes negative for β^- decay). The screening energy U_D for the temperature T (assuming the Debye-Hückel model is valid at these temperatures) is then $U_D = \sqrt{293 \text{ K}/T} \times U_e$. The correction of the decay constant λ depends on the decay mode. For β^+ , β^- , and electron capture (EC) Raiola *et al.* [1] assumed a $\lambda \approx E^5$ law, where E is the maximum energy of the β spectrum or the Q-value of the EC decay, respectively.

TABLE I. Predictions and measurements of half-life changes between room temperature and 12 K in different host metals where a significant change has been reported. The expectation for ^{196}Au in Au is also listed to be compared with our results.

Nuclide	Decay	Host	Theory	Measurement
^{22}Na	90% β^+	Pd	11%	$(1.2 \pm 0.2)\%$ [6]
^{198}Au	100% β^-	Au	−34%	$(-4.0 \pm 0.7)\%$ [7]
^{210}Po	100% α	Cu	3300%	$(6.3 \pm 1.4)\%$ [8]
^{196}Au	93% EC	Au	60%	—

For the α decay, the change of the decay constant is directly given by the penetrability. Therefore, the correction factor k for the half-life is

$$k = \left(\frac{E + U_D}{E + U_e} \right)^5, \quad \text{for } \beta^+, \beta^-, \text{ and EC, and}$$

$$k = \exp \left(\pi \eta(E) \frac{U_D - U_e}{E} \right), \quad \text{for } \alpha \text{ decay.}$$

For α decay, E is the energy of the emitted α and $\eta = Z_1 Z_2 \alpha / (v/c)$ is the Sommerfeld parameter, α the fine structure constant, and v the velocity.

We note here that the captured electron in the EC process is already at the position of the nucleus and does not penetrate a Coulomb wall. We therefore doubt the validity of the E^5 law to be applicable for EC. On the other hand, environmental electrons influence the wave function of the s-wave electrons. An extreme case of such an influence is the decay of ^7Be , the only radioactive nucleus with only s-wave electrons in the shell. Indeed, significant differences (about 1%) of the ^7Be lifetime have been observed, depending on the chemical environment. For other EC radionuclides thorough investigations exist with implantations in different host metals, see [18] and references therein. However, these well known half-life fluctuations are within to 1%. According to the Debye-Hückel model, 60% change is expected for ^{196}Au in Au cooled to 10 K.

The β decay screening can be described by an enhancement of the energy of the emitted β by replacing $P(E)$ (which is part of the Fermi function) by $P(E + U_D)$. However, even for very low energies the β particles must be treated relativistically and this simple picture of an “energy boost” fails. In a more detailed description [19] the Dirac or Klein-Gordon equation (if the spin plays no rule) must be solved for the Coulomb potential modified by the electron shell. This leads to the enhancement curves for the ^{22}Na decay shown in Fig. 1, for the $E_{\text{max}} = Q = 545$ -keV β^+ transition to the 1274-keV level of the ^{22}Ne daughter nucleus. The default Fermi function plus energy enhancement (as usually used for β decay analyses) can only be used for very small screening

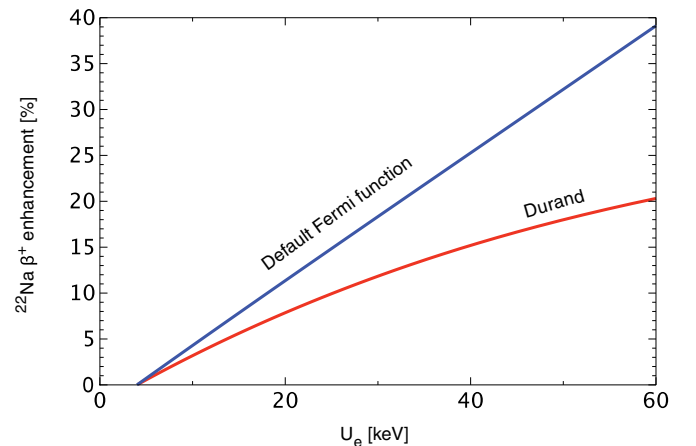


FIG. 1. (Color online) Screening enhancement vs screening energy U_e for the ^{22}Na β^+ decay. The screening model of Durand [19] should be taken for high screening energies.

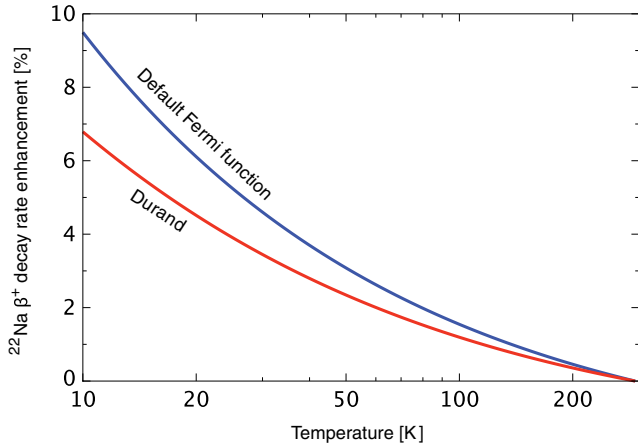


FIG. 2. (Color online) Enhancement of the ^{22}Na β^+ decay rate vs temperature. See also Fig. 1.

values. The corresponding temperature dependence, again assuming $U_D \approx 1/\sqrt{T}$, is shown in Fig. 2.

The Debye-Hückel model predicts a longer half-life for β^- and electron capture decay and a shorter half-life for β^+ and α decay [2,5]. The reported α decay change of 6% by ^{210}Po implanted in a metal at cryogenic temperatures [8] could not be confirmed by independent experiments studying other α -emitters [20–22], and there are also theoretical concerns regarding the Debye-Hückel model predictions for α decay [14]. In the present work we concentrate on an experimental study of β decay, where the predicted changes [2] have opposing signs for β^+ and β^- . Our aim is to check the validity of the predictions [1–5] of the Debye-Hückel model with a high-precision measurement for the two cases (^{22}Na and ^{198}Au) where previous experiments have reported a significant temperature dependence [6,7]. In addition, we study the temperature dependence of the half-life of ^{196}Au (EC).

IV. EXPERIMENTAL SETUP

A. Source production

We produced ^{22}Na by activation of ^{27}Al which is one of the metals with the highest screening energies [17] similar to Pd as used in the previous ^{22}Na study [6]. A 0.5 mm thick Al disk (3 cm diameter) was penetrated by 70-MeV protons from the TRIUMF main cyclotron, producing the desired isotope by fusion evaporation reactions on ^{27}Al deep in the Al lattice [23].

The ^{22}Na activity at the beginning of the decay measurement was 600 kBq.

^{196}Au (EC, $t_{1/2} = 6.2$ d) embedded in ^{197}Au was produced by exposing a sheet of gold (purity 99.95%, 16 mm \times 25 mm \times 0.5 mm) to bremsstrahlung from 12-MeV electrons, produced at the electron Linac ELBE, Forschungszentrum Dresden, Germany. One half of the activated gold sheet was mounted in a source calibration setup in the Forschungszentrum Dresden, the other half was shipped overnight to TRIUMF and mounted in the setup described below. The activity per sheet was 200 kBq plus a weak activation (6 kBq) of ^{198}Au .

^{198}Au (β^- , $t_{1/2} = 2.69$ d) embedded in ^{197}Au , was produced by exposing a sheet of gold (same properties as the ^{196}Au sample) to neutrons at the beam-stop of the TRIUMF TR13 cyclotron, resulting in an initial ^{198}Au activity of 200 kBq. ^{196}Au was also activated to 2 kBq (see also Sec. V).

B. γ -ray detection and cooling

Each of the activated samples was in turn fixed between two 6-mm thick copper blocks in thermal contact to the cold finger of a commercial, liquid-helium driven cryopump. The γ -rays emanating from the sample were observed by two high-purity germanium (HPGe) detectors (from hereon referred to as east and west detector), mounted outside the pump on opposite sides at 50 cm distance from the sample (Fig. 3). The cryopump as well as the detectors were fixed on a metal plate which in turn was mounted on massive stands, ensuring a mechanical stability of better than 0.1 mm. Moving the sample 0.1 mm horizontally toward one of the detectors would raise the counting rate by 0.04% but it would be noticeable in the second detector by a corresponding rate decrease. The thermal contraction of the cold finger (about 1 mm) leads to a vertical movement of the source, implying a change of the rate by less than 10^{-5} . The temperature was measured with a silicon diode, fixed in the middle of one of the copper blocks close to the source. The lowest temperature at this point was 8 ± 3 K when the cryopump was running. Prior to the measurement and cooling, the volume was evacuated with an oil-free scroll pump to 1.5 Pa.

The preamplified detector signals were each shaped by an amplifier (Ortec 671), gated by a constant fraction single channel analyzer (SCA), and digitized by a VME-ADC module (CAEN V785). The latter was triggered by the logical OR of both SCA outputs. The data acquisition system was

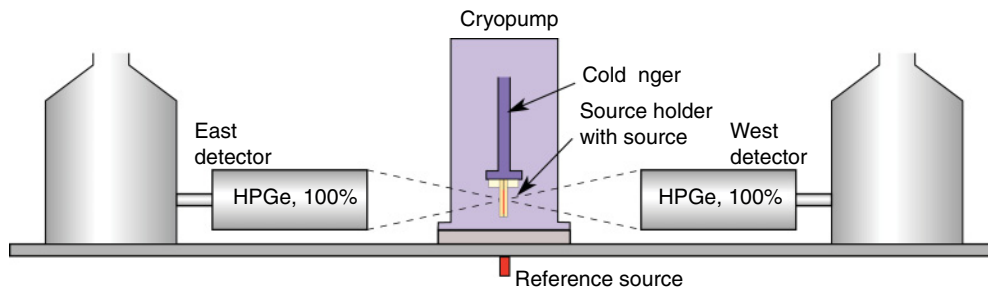


FIG. 3. (Color online) Schematic view of the experimental setup. The cryopump cooling the sample is situated between two HPGe detectors of 100% relative efficiency. All items were fixed on a common plate mounted on a stand.

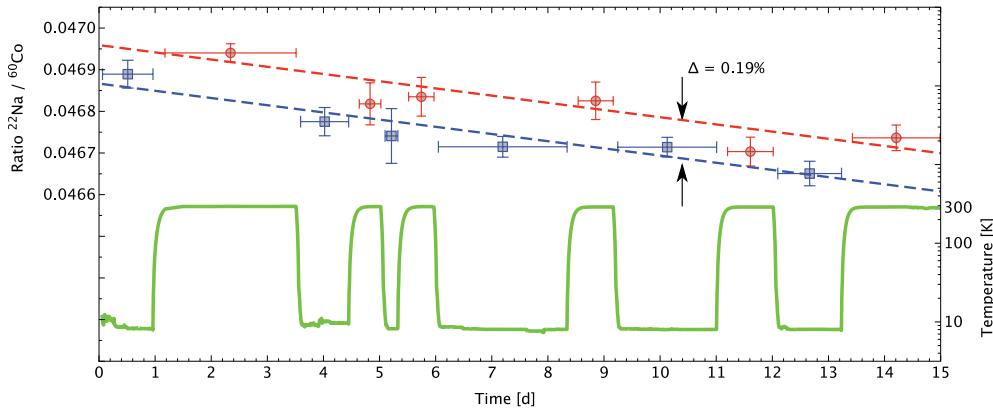


FIG. 4. (Color online) Counting rate of the ^{22}Na β^+ decay γ -rays relative to the ^{60}Co γ -ray rate, summed over both detectors. The vertical bars represent the statistical error, the horizontal bars the integration time. The temperature is also shown (right axis). The dashed lines are fits to the data points at room temperature (red circles) and at $T \approx 10$ K (blue squares) with the half-life of the ratio $^{22}\text{Na} / ^{60}\text{Co}$ fixed to the literature value. If not fixed, the resulting half-life of ^{22}Na is 2.57 ± 0.13 yr, in agreement with the literature value [24] of 2.60 yr.

recording each event as well as the signal from the temperature diode. Reference γ -ray sources were attached to the setup outside the cooling system (thus at room temperature), ^{60}Co for the ^{22}Na measurement and ^{137}Cs and ^{133}Ba for the ^{198}Au measurement. They have been selected according to their γ -ray energies so that energies above as well as below the γ -ray energy of the sample are available in the measured pulse height spectrum. This allowed to correct for the system's slightly energy-dependent dead-time and possible efficiency changes during the measurement, eliminating the major sources of uncertainty. As reference for the ^{196}Au measurement, a ^{54}Mn source (0.835 MeV) and a pulser (corresponding to 8.5 MeV) has been used for the Dresden setup (room temperature), and the ^{40}K background line (1.461 MeV) and a pulser (corresponding to 0.666 MeV and 1.403 MeV in the east and west detector, respectively) for the TRIUMF setup (12 K).

V. ANALYSIS AND RESULTS

For the peak integration several methods have been tested, including the GF3 algorithm [25]. However, they did not change the result compared with a simple linear background subtraction but complicated the automatic fitting of the few thousand spectra. We therefore applied a simple method with a constant interval around the each peak using the ROOT [26] data analysis framework.

A. ^{22}Na

Because of the long ^{22}Na half-life of 2.6 yr, only changes of the rate at 10 K compared with the rate at room temperature were measured. The sample was cooled and warmed up six times in cycles of about 2 d. The rate of the 1.275-MeV ^{22}Na γ -rays in each detector (22 s^{-1}) was normalized to the sum of the 1.173-MeV and the 1.333-MeV ^{60}Co γ -rays, corrected for the ^{22}Na and ^{60}Co decay with their nominal half-lives [24,27]. No significant difference could be observed between both detectors. However, the rate decreased by $0.19 \pm 0.04\%$ on the average when the sample was cooled (Fig. 4). This latter effect can be explained by a changed γ -ray transmission of the two 6-mm

thick copper blocks enclosing the source. The 0.33% thermal length contraction of copper at 10 K leads to a higher areal density, resulting in a lower γ -ray transmission by 0.18%, in agreement with the observed rate change. Therefore, the final ^{22}Na result corrected by the changed γ -ray transmission is $-0.02 \pm 0.06\%$ and $-0.01 \pm 0.05\%$ for the east and west detector, respectively. The fact that both numbers are consistent on the 0.06% level confirms the mechanical stability. East and west detector combined give a relative change of the ^{22}Na rate of

$$\Delta = (-0.01 \pm 0.04)\%.$$

B. ^{196}Au

The ^{196}Au measurement was not originally intended to be part of this experiment, therefore not much care has been taken to provide reference sources, and the error is one order of magnitude larger. As the measurement at room temperature has been performed with a different setup (in Dresden) than the measurement at 10 K (at TRIUMF), systematic errors do not cancel. However, the results are still clearly in contradiction to the prediction of 60% between room temperature and 10 K as it follows from the Debye-Hückel model. For the analysis, the 333-keV and 356-keV γ -ray lines have been used. The observed change of the half-life is

$$\Delta = (+0.1 \pm 0.3 \pm 0.2)\%.$$

The second error is a systematic uncertainty that has been observed when normalizing the TRIUMF measurement to the pulser or to the K-40 background rate.

C. ^{198}Au

For ^{198}Au , benefiting from the short half-life of 2.7 d, a direct measurement of the exponential decrease of the rate and therefore the half-life has been performed, running the setup for three half-lives (8 d). However, as the rate changes by one order of magnitude dead-time corrections must be done very carefully. We developed a pulse-height dependent dead-time model based on the electronic behavior of the

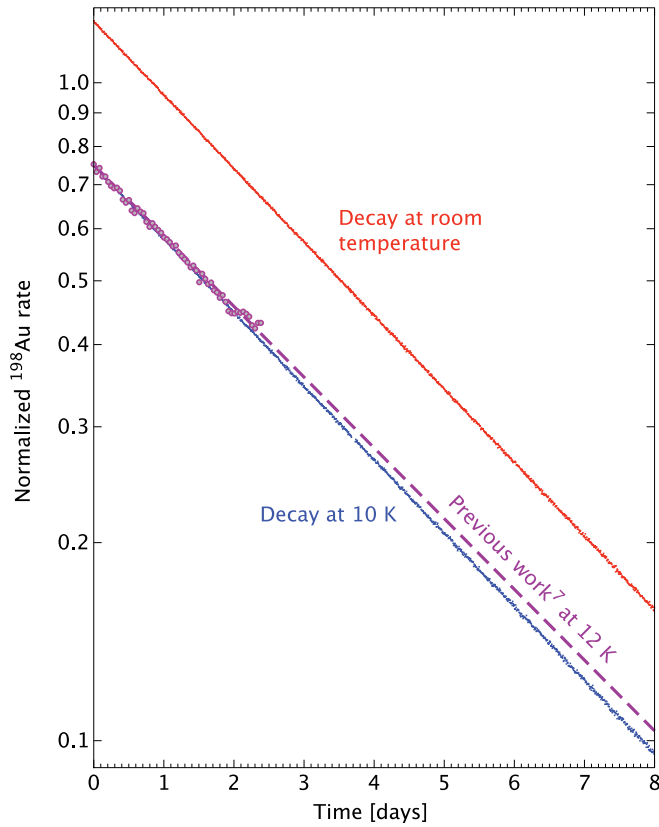


FIG. 5. (Color online) Decrease of the 412-keV ^{198}Au γ -ray intensity at room temperature and at 10 K, relative to the half-life corrected γ -ray intensities of ^{133}Ba and ^{137}Cs . Each point corresponds to a 10-min integration interval. The normalized data points (big circles) from the previously reported longer half-life [7] and the corresponding calculated decay curve (dashed) is also indicated and clearly disagrees with our data.

V785 ADC as described in the manual combined with the Poisson distribution of the pulses within the gate time window of 16 μs . Sum peaks could be observed in the spectra as well but they turned out to be negligible. The model was then checked against the 0.276-MeV, 0.303-MeV, and 0.384-MeV γ -ray lines of the ^{133}Ba and the 0.662-MeV line from the ^{137}Cs reference source and all intensities showed the same time dependence after correction, compatible with the half-life of

TABLE II. Precise (error < 0.005 d) measurements of the ^{198}Au half-life since 1969.

Nr.	Year	Half-life (d)	Reference
1	1969	2.695(2)	Vuorinen and Kaloinen [30]
2	1970	2.696(4)	Costa Paiva and Martinho [31]
3	1970	2.6946(10)	Cabell and Wilkins [32]
4	1980	2.6935(4)	Rutledge <i>et al.</i> [33] (based on a reanalysis of Merritt and Gibson [34])
5	1982	2.695(2)	Hoppes <i>et al.</i> [35]
6	1990	2.6966(7)	Abzouzi <i>et al.</i> [36]
7	1992	2.69517(21)	Unterweger [37]
8	2004	2.69573(14)	Unterweger and Lindstrom [38]
9	2005	2.6924(11)	Lindstrom <i>et al.</i> [39]
10	2008	2.6949(8)	Goodwin <i>et al.</i> , 293 K [28]
11	2008	2.6953(9)	Goodwin <i>et al.</i> , 19 K [28]
12	2008	2.6971(20)	Kumar <i>et al.</i> , 293 K [29]
13	2008	2.6976(23)	Kumar <i>et al.</i> , 12.5 K [29]
14	2008	2.6939(4)	This measurement, 293 K
15	2008	2.6935(5)	This measurement, 10 K

10.5 yr and 30.1 yr, respectively. The most intense ^{133}Ba line at 356.0 MeV was excluded from the analysis as it could not be separated from the most intense line at 355.7 MeV emanating from ^{196}Au impurities ($t_{1/2} = 6.2$ d). The ^{198}Au 0.412-MeV γ -ray rate normalized to the sum of the aforementioned ^{133}Ba and the 0.662-MeV ^{137}Cs γ -ray rate is shown in Fig. 5. The result for the ^{198}Au half-life averaged over both detectors is 2.6939 ± 0.0004 d at room temperature and 2.6935 ± 0.0005 d at 10 K, therefore the relative half-life change for ^{198}Au embedded in ^{197}Au when cooled to 10 K is

$$\Delta = (-0.015 \pm 0.025)\%.$$

This ‘zero’ is in agreement with the recently published result from Goodwin [28] of $\Delta = (0.015 \pm 0.045)\%$ where the sample was cooled to 19 K, and Kumar [29] with $\Delta = (0.02 \pm 0.11)\%$ where the sample was cooled to 12.5 K.

As no temperature dependence could be observed, both results can be concatenated to 2.6937 ± 0.0003 d. This is 0.06%(5 σ) below the recommended NIST value of 2.6952 ± 0.0002 d [27,37] but in excellent agreement with the

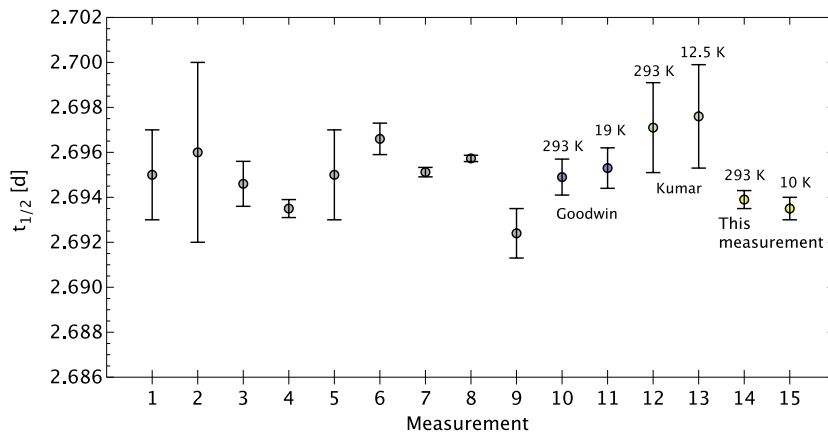


FIG. 6. (Color online) Precise (error < 0.005 d) measurements of the ^{198}Au half-life since 1969, see Table II.

high-precision measurement [33]. The recommended value [27,37] seems to be based on a reanalysis of [35] rather than a weighted mean of previous measurements where it remains unclear what exactly was changed in the analysis. The Goodwin measurement [28] is in good agreement with our result with a similar error, and the authors performed extensive dead-time measurements with different sources. Table II and Fig. 6 show measurements of the last 40 years with an error less than 0.005 d, so it seems a reevaluation of the recommended half-life is called for.

VI. CONCLUSION

Compared to previous half-life change measurements [6,7], the present results have a factor of 5 better uncertainty for the ^{22}Na half-life change and a factor of 30 better uncertainty for the ^{198}Au half-life change. Our results are in disagreement (Table I) both with the previous experiments [6,7] and with the predictions from the Debye-Hückel model [1–5]. The host metal for our ^{22}Na measurement was different (Al instead of Pd [6]), and it is conceivable that the previously reported half-life change [6] was very specific to Pd. However, our production of the ^{198}Au sample was not significantly different from previous work [7] with a strikingly different result. Two recent measurements [28] and [29], had the same goal the same goal to double-check the [7] measurement, and the result

is the same as ours. As a side effect, we could contribute a high-precision value for the absolute ^{198}Au half-life.

Concluding, the present data rule the Debye-Hückel model inapplicable for β emitters embedded in metals, on the level of 0.04% precision. The previously reported half-life changes for β decay [6,7] seem to be erroneous. Returning to the motivation of the present study, the unexpectedly high experimental values for the electron screening effect [13,17] in the case of deuterium embedded in metals remain an intriguing and so far unexplained [9] fact. The present data show that the previously suggested explanation by the Debye-Hückel model [1–5] does not pass a stringent test of its predictions, so physicists working on understanding this phenomenon are back to square one.

ACKNOWLEDGMENTS

We thank Peter Machule and Dave Ottewell (TRIUMF) for the technical support, Clint LaForge and Gordon Ball (TRIUMF) for providing the cryopump and the detectors, respectively, and Andreas Hartmann (FZD) for testing Au activation methods. We also thank Konrad Czerski (University of Szczecin, Poland), Armin Huke (Technische Universität Berlin, Germany), Dave Hutcheon, Pat Walden, and Mike Trinczek (TRIUMF) for the enlightening discussions. We finally thank the TRIUMF data acquisition group for providing the electronics.

-
- [1] F. Raiola *et al.*, J. Phys. G **31**, 1141 (2005).
 - [2] K. U. Kettner, H. W. Becker, F. Strieder, and C. Rolfs, J. Phys. G **32**, 489 (2006).
 - [3] C. Rolfs, Nucl. Phys. News **16**, 9 (2006).
 - [4] Ph. Ball, Nature News, Columns Blogs (2006).
 - [5] H. Muir, New Scientist **2574**, 36 (2006).
 - [6] B. Limata *et al.*, Eur. Phys. J. A **28**, 251 (2006).
 - [7] T. Spillane *et al.*, Eur. Phys. J. A **31**, 203 (2007).
 - [8] F. Raiola *et al.*, Eur. Phys. J. A **32**, 51 (2007).
 - [9] E. Salpeter, Aust. J. Phys. **7**, 373 (1954).
 - [10] W. Debye and E. Hückel, Phys. Z. **24**, 185 (1923); **24**, 305 (1923).
 - [11] K. Czerski, P. Heide, A. Huke, L. Martin, and G. Ruprecht, in *Proceedings of the International Symposium on Nuclear Astrophysics, Nuclei in the Cosmos IX, CERN, Geneve, 2006*, PoS(NIC-IX)044, p. 318.
 - [12] K. Czerski, A. Huke, P. Heide, M. Hoefft, and G. Ruprecht, *Proceedings of the International Symposium on Nuclear Astrophysics, Nuclei in the Cosmos V, Volos, Greece, 1998* (Editions Frontières, 1998), p. 152.
 - [13] K. Czerski, A. Huke, P. Heide, and G. Ruprecht, Europhys. Lett. **68**, 363 (2004).
 - [14] N. T. Zinner, Nucl. Phys. A **781**, 81 (2007).
 - [15] T. S. Wang *et al.*, J. Phys. G **34**, 2255 (2007).
 - [16] A. Huke, K. Czerski, G. Ruprecht, N. Targosz, W. Żebrowski, and P. Heide (accepted for Phys. Rev. C, 2008).
 - [17] F. Raiola *et al.*, Eur. Phys. J. A **19**, 283 (2004).
 - [18] Y. Nir-El *et al.*, Phys. Rev. C **75**, 012801(R) (2007).
 - [19] L. Durand *et al.*, Phys. Rev. B **135**, 310 (1964).
 - [20] H. B. Jeppesen *et al.*, Eur. Phys. J. A **32**, 31 (2007).
 - [21] N.-J. Stone *et al.*, Nucl. Phys. A **793**, 1 (2007).
 - [22] N. Severijns *et al.*, Phys. Rev. C **76**, 024304 (2007).
 - [23] S. Lapi, master thesis, Simon Fraser University, Burnaby, B. C., Canada (2003).
 - [24] R. B. Firestone, Nucl. Data Sheets **106**, 1 (2005).
 - [25] RADWARE GF3 algorithm, <http://radware.phy.ornl.gov/gf3>.
 - [26] ROOT data analysis framework, <http://root.cern.ch>.
 - [27] Z. Chunmei, Nucl. Data Sheets **95**, 59 (2002).
 - [28] J. R. Goodwin, V. V. Golovko, V. E. Jacob, and J. C. Hardy, Eur. Phys. J. A **34**, 271 (2007).
 - [29] V. Kumar *et al.*, Phys. Rev. C **77**, 051304(R) (2008).
 - [30] A. Vuorinen and E. Kaloinen, Ann. Acad. Sci. Fenn., Ser. A6 **310**, 5 (1969).
 - [31] M. M. Costa Paiva and E. Martinho, Int. J. Appl. Radiat. Isot. **21**, 40 (1970).
 - [32] M. J. Cabell and M. Wilkins, J. Inorg. Nucl. Chem. **32**, 1409 (1970).
 - [33] A. R. Rutledge, L. V. Smith, and J. S. Merritt, At. Energy Can. Ltd., Rep. AECL-6692 (1980).
 - [34] J. S. Merritt and F. H. Gibson, At. Energy Can. Ltd., Rep. AECL-5802 (1977), p. 43.
 - [35] D. D. Hoppes *et al.*, National Bureau of Standards, Rep. NBS-SP 626 (1982), p. 85.
 - [36] A. Abouzouzi *et al.*, J. Radiol. Nucl. Chem. **144**, 359 (1990).
 - [37] M. P. Unterweger, D. D. Hoppes, and F. J. Schima, Nucl. Instrum. Methods A **312**, 349 (1992).
 - [38] M. P. Unterweger and R. M. Lindstrom, Applied Radiation and Isotopes **60**, 325 (2004).
 - [39] R. M. Lindstrom, M. Blaauw, and M. P. Unterweger, J. Radiol. Nucl. Chem. **263**, 311 (2005).